Novel aerial photography as an aid to sampling secondary structure in pine stands

Pat Teti

Mountain Pine Beetle working paper 2009-16

Natural Resources Canada
Canadian Forest Service
Pacific Forestry Centre
506 West Burnside Road
Victoria, BC V8Z 1M5
Canada

MPBP Project # 7.23

© Her Majesty the Queen in right of Canada 2009
Printed in Canada

Library and Archives Canada Cataloguing in Publication

Teti, Patrick Anthony, 1949-
Novel aerial photography as an aid to sampling secondary structure in pine stands
/ Pat Teti.

(Mountain pine beetle working paper ; 2009-16)
"MPBP Project # 7.23".
Includes abstract in French.
Available also on the Internet.
Includes bibliographical references.
ISBN 978-1-100-13393-5
Cat. no.: Fo143-3/2009-16E

1. Mountain pine beetle--British Columbia. 2. Lodgepole pine--Diseases and pests--British Columbia. 3. Conifers--Remote sensing--British Columbia. 4. Understory plants--Remote sensing--British Columbia. 5. Forest surveys--British Columbia. 6. Aerial surveys in forestry--British Columbia. I. Pacific Forestry Centre II. Title. III. Series: Mountain Pine Beetle Initiative working paper 2009-16

SB945 M78 T47 2009 **634.9'7516768** **C2009-980193-0**

Abstract

This project describes a new method for sampling secondary structure in beetle-attacked pine stands and reports on a test of its accuracy. The method consists of interpreting aerial photos taken when snow covers the forest floor and the sky is overcast.

Winter/overcast aerial photos of beetle-attacked, pine-leading test plots in British Columbia, Canada, were acquired with a digital SLR camera in March 2008, geo-referenced to provincial orthophotos, and interpreted for secondary structure numbers, locations, and sizes. The resulting stem maps were field-checked for accuracy in the summer and fall of 2008. Tree classification tests consisted of determining whether each interpreted tree was in the plot, whether it was a green conifer, and whether any green conifers in the plot were missed. Net errors in counting secondary structure stems ranged from +3% to +21% in four plots; the most common error was the misclassification of dead pine trees or brush as green conifers. The diameters of green conifer crowns were also measured on the aerial photos and field-checked. Photo-interpreted crown diameters averaged 38 cm less than actual crown diameters, with 78% of the variance explained.

As these accuracies are based on field-checking only four plots, they are preliminary; however, the results provide the first known demonstration that secondary structure can be interpreted on winter/overcast aerial photos. We conclude that this method can provide useful information on secondary structure at a rate of coverage, cost per unit area, and accuracy suitable for many applications if field-checking is used for training and verification.

Keywords: Mountain pine beetle, winter aerial photography, lodgepole pine, secondary structure

Résumé

Le projet décrit une nouvelle méthode de prélèvement de structure secondaire dans les peuplements de pins attaqués par le dendroctone et rend compte d'un essai portant sur son exactitude. La méthode consiste à interpréter des photos aériennes prises lorsque la neige couvre le sol de la forêt et que le ciel est nuageux.

Des photos aériennes prises en hiver, sous un ciel nuageux, de parcelles d'essai dominées par des pins attaqués par le dendroctone en Colombie-Britannique, au Canada, ont été prises au moyen d'un appareil mono-objectif réflex numérique en mars 2008, géoréférencées en orthophotographies provinciales et interprétées quant au nombre de structures secondaires, à leur situation et à leur taille. L'exactitude des cartes qui en ont résulté a été vérifiée sur le terrain durant l'été et l'automne 2008. Des tests de classification des arbres ont permis de déterminer si chaque arbre interprété se trouvait sur la parcelle, s'il s'agissait d'un conifère vert et si des conifères verts sur cette parcelle étaient manquants. Les erreurs de décompte des tiges de structures secondaires allaient de +3 à +21 % sur quatre parcelles, le type d'erreur le plus courant étant une mauvaise classification de pins décimés ou de buissons, identifiés comme des conifères verts. Le diamètre des couronnes des conifères verts a également été mesuré sur les photos aériennes et contrôlé sur le terrain. Le diamètre donné par les photos était en moyenne inférieur de 38 cm au diamètre réel de la couronne, avec 78 % de variation expliquée.

Étant donné que ces pourcentages d'exactitude se fondent sur le contrôle sur le terrain de quatre parcelles seulement, ils ne sont que préliminaires; cependant, ces résultats sont la première démonstration reconnue que la structure secondaire peut être interprétée sur des photos aériennes prises en hiver, sous un ciel nuageux. Nous en concluons que cette méthode peut fournir des renseignements utiles sur la structure secondaire avec un taux de couverture, un coût par zone unitaire et une exactitude adaptés pour une variété d'applications, si le contrôle sur le terrain est utilisé à titre d'exercice et de vérification.

Mots clés: dendroctone du pin ponderosa, photographie aérienne en hiver, pin tordu latifolié, structure secondaire

Table of Contents

Abstract iii

Table of Contents iv

List of Tables v

List of Figures v

1 Introduction 1
- 1.1 Overview 3

2 Materials and Methods 3
- 2.1 Site selection and image capture 3
- 2.2 Spatial data processing 4
  - 2.2.1 Flight line mapping 4
  - 2.2.2 Georeferencing aerial photos 5
  - 2.2.3 Creating vector data for plots 6
- 2.3 Interpreting photos 7
- 2.4 Field data collection 8
- 2.5 Analysis 8

3 Results 9
- 3.1 Discrimination of secondary structure 9
- 3.2 Classification and mapping of secondary structure 10
- 3.3 Estimation of crown diameters 15
- 3.4 Horizontal scale accuracy 19
- 3.5 Operational considerations 19

4 Discussion and Conclusions 20
- 4.1 Detection, classification, and mapping of secondary structure 20
- 4.2 Crown diameters estimated on aerial photos 20
- 4.3 Results in relation to the secondary structure regulation 23
- 4.4 Software platform and interpretation methods 23

5 Acknowledgements 23

6 Contact 24

7 Literature Cited 24

List of Tables

Table 1. Plot information and summary of secondary structure classification accuracy 15

List of Figures

Figure 1. Cropped and registered aerial photos of forest in the IDFdk3 taken in: (a) summertime under clear skies, (b) winter under overcast skies, and (c) winter under clear skies. Species and heights of live residual conifers from field data are superimposed on (d). Most unlabelled trees are dead pine. 2
Figure 2. Sites selected for testing (circles) and full field-checking (labelled circles) 4
Figure 3. Google Earth screen captures of (a) a ground target, the March 1st, 2008 flight track, and calculated locations of the aircraft corresponding with photos, and (b) March 1st photo #7316 visually georeferenced onto the provincial orthophoto 6
Figure 4. Two sequential, overlapping images of the northeast quadrant of plot SS03 arranged for viewing in stereo. 7
Figure 5. A portion of plot SS04 taken during summer/clear, winter/overcast, and winter/clear conditions 10
Figure 6. Plot SS01 reference image. 11
Figure 7. Plot SS01 map of interpreted green conifers and errors of commission and omission. 11
Figure 8. Plot SS02 on reference image. 12
Figure 9. Plot SS02 map of interpreted green conifers and errors of commission and omission. 12
Figure 10. Plot SS03 on reference image. 13
Figure 11. Plot SS03 map of interpreted green conifers and errors of commission omission. 13
Figure 12. Plot SS04 on reference image. 14
Figure 13. Plot SS04 map of interpreted green conifers and errors of commission and omission 14
Figure 14. Tree crown diameters measured in the field versus those measured on the georeferenced aerial photo in Google Earth in plots SS01 through SS04 16
Figure 15. Tree crown diameters measured in the field versus those greater than 1 m as measured on the aerial photos with data from plots SS01 through SS04 merged 17
Figure 16. Field- versus photo-measured crown diameters for trees with crowns $\leq$ 1 m diameter in plots SS02 (a), SS03 (b), and SS04 (c) 18
Figure 17. Distances between ground features on the four plots made in the field (y) and estimated on the georeferenced aerial photos (x).. 20
Figure 18. Comparison of crown diameters measured in the field by one crew in October 2008 and by another in May 2009.. 21
Figure 19. Cropped images of some understorey fir and spruce trees in plots SS01 (top row) through SS04 (bottom row) showing diameters of individual crowns measured on photos (smaller arrows) and in the field (larger arrows). 22

1 Introduction

In the aftermath of the current mountain pine beetle epidemic, renewed attention is being paid to understorey and larger trees that are likely to survive in attacked stands, i.e. *secondary structure* (Coates et al. 2006). For example, the Forest Planning and Practices Regulation now requires that secondary structure be retained during pine salvage logging operations in certain Timber Supply Areas if it is present in sufficient quantity (see secondary structure surveys at http://www.for.gov.bc.ca/hfp/silviculture/Silviculture_Surveys.html.) Non-timber values such as hydrology and biodiversity may also be enhanced by preferentially retaining beetle-attacked pine stands that contain secondary structure at amounts that are lower than the regulatory threshold (Coates et al. 2006). For these reasons, more data on secondary structure in beetle-attacked pine stands is urgently needed (de Montigny et al. 2007). Ground surveys yield the best quality information but the time required and cost per unit area could limit their application. Therefore, it would be advantageous to have a complementary method of data collection that can produce secondary structure data at a faster rate and lower cost.

Aerial photography and satellite imagery are crucial sources of information for forest inventory but standard remote sensing products are not well suited to providing direct information about understorey trees. As noted by Coates et al. (2006),

> We currently have limited information on the abundance of seedlings and saplings (understorey trees) in pine-leading stand types. This information is difficult to obtain from traditional inventory data.

It is difficult to quantify secondary structure using standard remote sensing products because sub-metre resolution is required and because understorey trees are hard to see even if the resolution is sufficient, for three reasons:

1. taller trees partially obscure them,
2. they have similar reflectance as the forest floor, and
3. shadows cast by the overstorey illuminate them unevenly.

To an airborne sensor, a sparsely foliated or defoliated forest canopy exhibits characteristics of a cloud in that it is composed of discontinuous sub-pixels sized elements. As such, the degree to which it obscures a darker background varies with illumination. Therefore, a defoliated pine canopy most obscures secondary structure when it is illuminated by direct sunlight, particularly when the secondary structure is shaded. These factors can seriously limit our ability to detect understorey trees on aerial images but they can be reduced by winter/overcast aerial photo acquisition.

Figure 1a shows a small portion of an aerial photo of a pine-leading stand in the IDFdk3. The photo was taken in July 2008 and represents a typical aerial photo taken under clear skies during the growing season. The site is in a polygon mapped as 92% pine, 60 years old, 11 m tall, and with 10% crown closure. Red and grey pine crowns are visible and there is evidence of green tree crowns. However, further interpretation without the use of stereo would be difficult. Figure 1b shows the same portion of ground on a photo taken in March 2008 when snow covered the forest floor and the sky was overcast. Figure 1c is part of an aerial photo of the same area under winter/clear conditions. Figure 1d shows the results of field-checking the site in the summer of 2009. This figure shows that understorey spruce trees are much more obvious on the photo taken during winter/overcast conditions than on the summer photo.

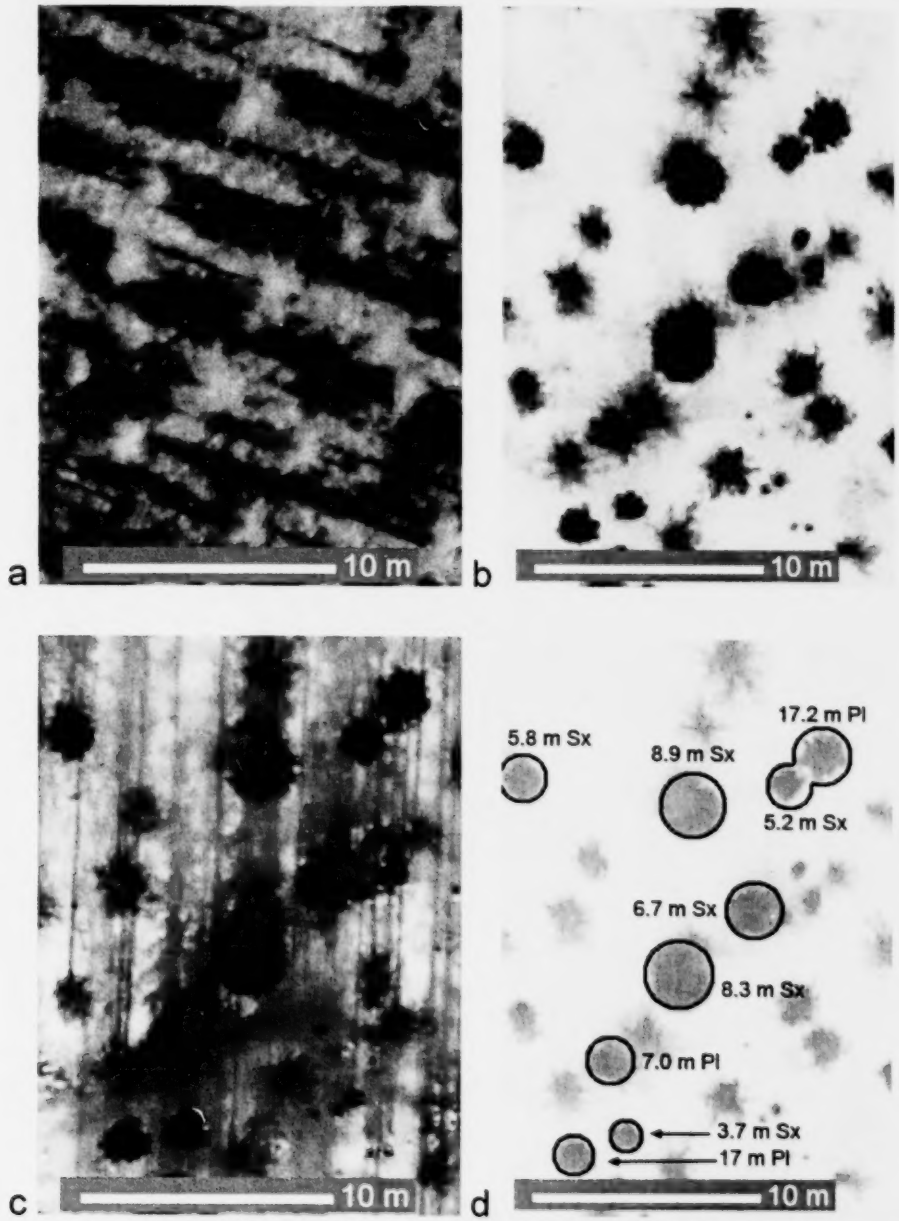

Figure 1. Cropped and registered aerial photos of forest in the IDFdk3 taken in: (a) summertime under clear skies; (b) winter under overcast skies; and (c) winter under clear skies. Species and heights of live residual conifers from field data are superimposed on (d). Most unlabelled trees are dead pine.

Winter/overcast imagery has three important advantages:

1. If a dead pine crown is directly above an understorey tree, its sub-pixel sized features interfere much less with the visibility of the dark understorey tree than if the pine crown is illuminated by direct sunlight.
2. When snow covers the forest floor and the trees have shed any intercepted snow, green conifer crowns have much lower reflectance than the background.
3. When the sky is overcast, illumination is relatively uniform, which allows pixel values to represent feature properties rather than variations in illumination.

The net effect is that on winter/overcast aerial photos, pixels representing understorey spruce crowns are consistently darker than pixels representing the background. These advantages are enhanced by the presence of a defoliated overstorey because the vertical projections of understorey fir and spruce crowns tend be larger, rounder, and denser.

1.1 Overview

This report describes the results of a preliminary accuracy test of sampling secondary structure by interpreting aerial photos taken during winter overcast conditions.

Overlapping sequential photos of previously selected plots were georeferenced, plot geometry was overlaid, photos were interpreted, and the accuracy of interpretation was determined by field checking. The accuracy of tree classification was assessed by determining errors of omission and commission for each tree based on whether it was correctly defined as inside the plot and whether it was a green conifer. The accuracy of measuring crown diameters of green conifers was also assessed by direct comparison of field and photo measurements.

Photo interpretation consisted of attempting to identify every green conifer in a plot, determining its x,y-coordinates to the nearest 10 cm, and measuring its crown diameter to within 10 cm. The photo interpreters concluded that the combination of the uniform white background of snow on the forest floor and diffuse lighting from an overcast sky greatly improved their ability to interpret secondary structure in beetle-attacked pine stands.

Residual green conifers included pine, fir, and spruce trees. Net errors in counting them on aerial photos ranged from +3% to +21%, indicating that commission errors exceeded omission errors. Crown diameters of green conifers estimated on georeferenced aerial photos were well correlated with those measured on the ground ($r^2 = 0.78$) and were underestimated by averages of 0.26 to 0.56 m in the four plots.

This aerial photo acquisition method provides good quality images of understorey fir and spruce in beetle-attacked pine stands. It demonstrates that stem maps can be made and crown diameters can be estimated with an accuracy that is sufficient for purposes such as stratification before field sampling and for research. The number of field-checked plots is too small to support reliable conclusions about accuracy but is sufficient to present the concept and discuss possible applications. The method's potential to provide information on secondary structure faster and cheaper than relying on ground sampling enhances its value.

2 Materials and Methods

2.1 Site selection and image capture

An initial sample of 16 test sites was established based on high pine beetle attack status, a diversity of secondary structure, overlap with Permanent Sample Plots, and proximity to Williams Lake (Figure 2). All field-checked plots are in the Central Cariboo Forest District in beetle-attacked stands of 80% to 100% lodgepole pine aged 60 to 128 years.

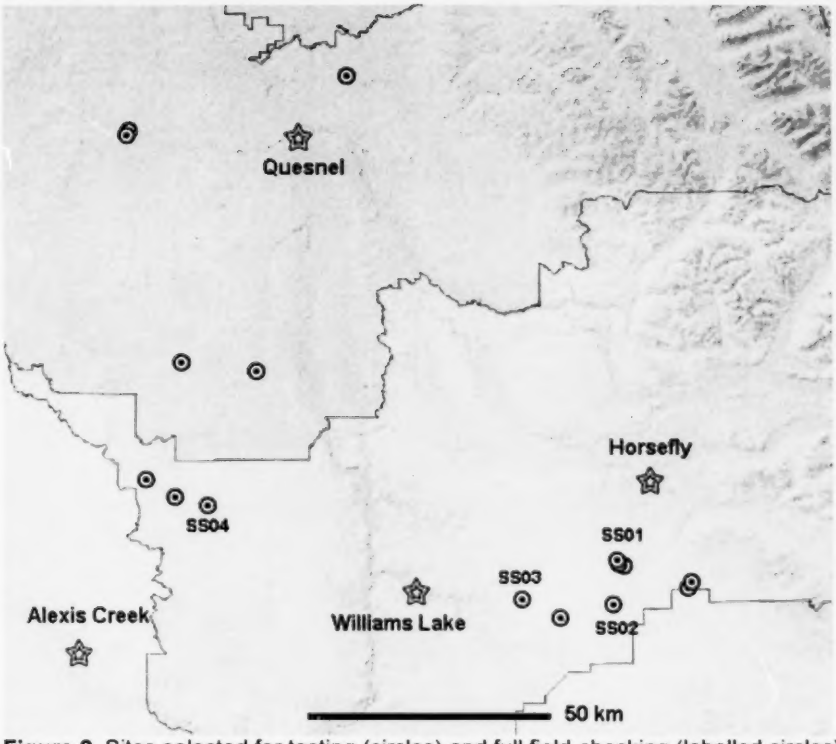

Figure 2. Sites selected for testing (circles) and full field-checking (labelled circles).

Aerial photos for interpretation were taken in March 2008, the summer of 2008, and late winter of 2009 to compare photos taken under different conditions and to detect changes over time.

All flights were made in a chartered Cessna 206 with a camera port in the floor. Navigation to targets was by recreational GPS receivers (Garmin 76). Photos were taken with a digital SLR camera (Nikon D200, 3872 x 2592 pixels, with 105 mm micro Nikkor or 60 mm Nikkor lens). The camera was mounted vertically over the port on a vibration-dampening suspension and was oriented such that the direction of travel was toward the top of the photo. Heights above ground were planned so that the width of photo coverage was approximately 200-300 m with a pixel size of 5-8 cm on the ground. Photos were taken at 1- or 2-second intervals with an electronic remote shutter release (Nikon MC-36). The resulting overlap between sequential images was at least 30%.

2.2 Spatial data processing

2.2.1 Flight line mapping

Flight lines were recorded on GPS and downloaded. The data format is a series of connected line segments where each node is defined by a geographic coordinate (x,y,z) and a precise GPS satellite time. All digital photos also had a time stamp with 1-s resolution, enabling the location of every photo to be interpolated based on the GPS track and jpeg file time stamp. An average time difference between camera time and GPS time was calculated for each flight by taking photos of the GPS time display and reading the corresponding times from the photo and the jpeg files. Photo centres were automatically approximated with GPS Photo Link software and the resulting photo points imported into Google Earth.

The accuracy of calculated photo nadirs was limited by the accuracy of the flight track nodes and by the synchronization of jpegs to no finer than the nearest second. At a ground speed of 55 m/s,

this could result in a systematic error in time and space of up to two seconds or 110 m along the flight track. The other source of uncertainty is the recreational GPS positions themselves.

2.2.2 Georeferencing aerial photos

The brightness and contrast of photos were adjusted in Adobe Photoshop using the Levels tool to optimize interpretation on a computer screen. Some images were colour-enhanced to bring out shades of green and red.

Photos were georeferenced as follows. By referring to the flight line map in Google Earth, photo numbers over a target were identified and photos were inspected to determine the one whose nadir was closest to the plot centre. That photo was generally selected as the photos that would be interpreted (the "reference photo"). That photo was imported as an image overlay into Google Earth and was visually registered to the orthophoto using at least three control points which were ground features (e.g., coarse woody debris) where possible or, alternatively, tree crowns.

Depending on the footprints of adjacent aerial photos, either one or two overlapping photos were imported as overlays and were correlated to the reference photo using at least three ground control points, which were usually coarse woody debris. The resulting set of two or three georeferenced photos were named according to the image numbers, the reference photo was identified, and the folder of images was saved as a Google Earth kmz file.

When features on an individual aerial photo were too small to match to the underlying orthophotos, a strip mosaic of three or more overlapping subsampled images was made with Panorama Tools software. This increased the image footprint enough to overlap distinctive features on the landscape. The strip mosaic was imported into Google Earth and georeferenced according to the procedure described above. Full-resolution aerial photos were then overlaid and registered to the strip mosaic.

An important outcome of georeferencing an image is the resulting horizontal scale, because plot boundaries and crown diameter measurements on the aerial photos depend on it. Therefore, the accuracy of the horizontal scale on each georeferenced photo was checked in the field as discussed in the Results section.

Figure 3a shows an aerial photo target, the GPS track from March 1, 2008, and the calculated flight line map superimposed on the BC Government orthophoto as viewed in Google Earth. Figure 3b shows the March 1st aerial photo that was selected as the reference photo after being georeferenced onto the orthophoto.

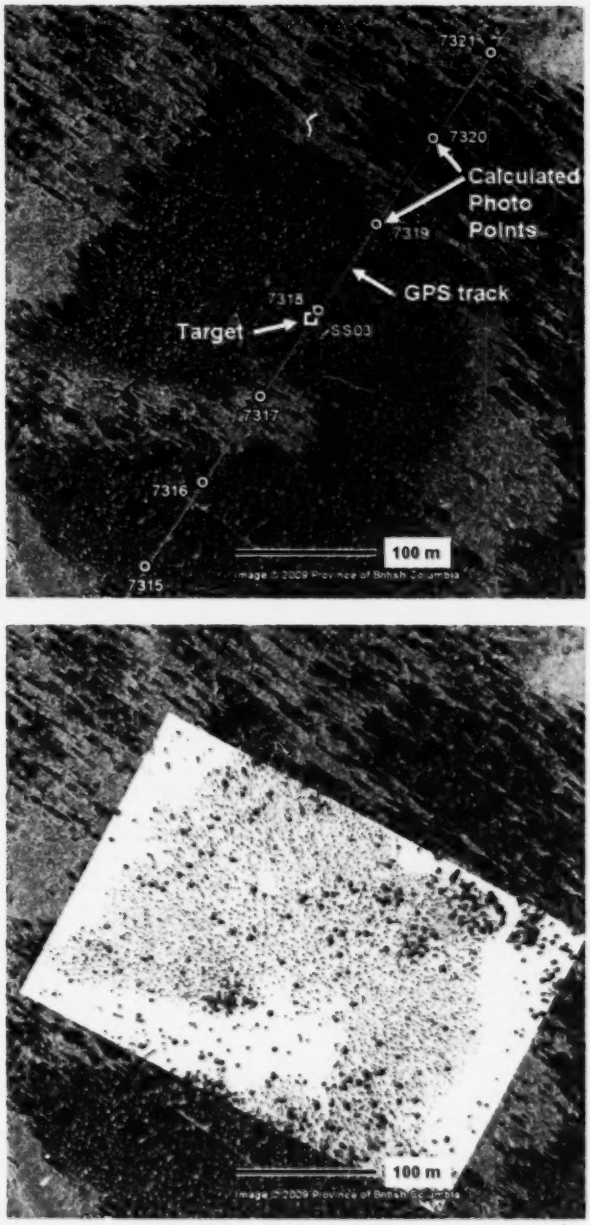

Figure 3. Google Earth screen captures of (a) a ground target, the March 1st, 2008 flight track, and calculated locations of the aircraft corresponding with photos, and (b) March 1st photo #7316 visually georeferenced onto the provincial orthophoto.

2.2.3 Creating vector data for plots

Plots were defined on the georeferenced photos as follows. A distinctive tree which had a clear germination point and which could later be found in the field was selected as the plot centre and a point was created in Google Earth. A circular plot of ¼ ha was projected around that point by

importing plot centres into Global Mapper, creating *range rings* of 28.2 m radius, and saving in kmz format. Each plot was divided into quadrants with east-west and north-south boundaries as shown in Figures 6 through 13. The total area that was field-checked consisted of two or three quadrants in each plot, i.e., 1250 or 1875 sq. m.

2.3 Interpreting photos

Photo interpretation was done by either a registered professional forester (R.P.F.) or an R.P.F. qualified as a Vegetation Resource Inventory (VRI) interpreter. Each plot was interpreted on the georeferenced reference image. Adjacent images were used to interpret depth by alternately viewing the reference image and one of the adjacent images rather than by binocular stereopsis. These images could have been made into stereo pairs but were instead viewed one at a time in registration with each other, which adequately revealed parallax associated with tree height. Google Earth is well-suited for this due to its fast and simple controls for zooming, panning, and for turning image layers on and off. Figure 4 shows an example of two such images for the northeast quadrant of plot SS03. They have been rotated with the direction of flight running from left to right on the page so that they can be viewed as a stereo pair. However, when interpreted in Google Earth, they were viewed one at a time as registered layers, a procedure that transfers poorly to the printed page.

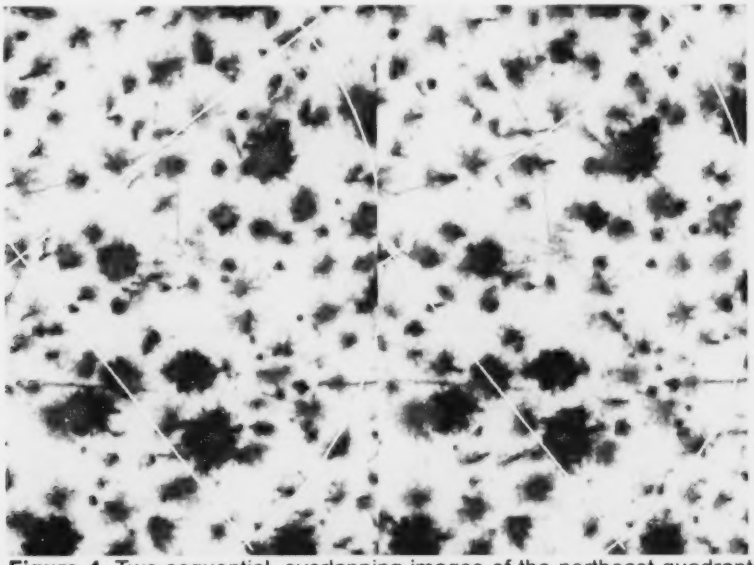

Figure 4. Two sequential, overlapping images of the northeast quadrant of plot SS03 arranged for viewing in stereo.

Stems were mapped by assigning a number and location to each tree identified as a residual green conifer. A tree was judged inside a plot based on its germination point on the reference photo. If the germination point was on the plot boundary, it was called in or out by a coin flip. In addition to horizontal scale accuracy, pinpointing a tree's location was also important because it formed the basis for calculating stems per hectare.

The crown diameter of each secondary structure stem was estimated to the nearest 10 cm using the Google Earth ruler tool. The resulting measurement was entered into the description field of

the corresponding point. Photo-interpreted data were converted to CSV format using Global Mapper software for later analysis in MS Excel. Dead pine trees were not interpreted.
All photo interpretation decisions were made while alternately viewing two or three sequential and overlapping images, which greatly aided in locating germination points and in identifying crown perimeters.

2.4 Field data collection

After stem mapping, aerial photo prints (with coverage like Figure 4 and resolution like Figure 1b) were checked in the field. The first step consisted of navigating to the plot by recreational GPS and then finding the tree that had been selected as the plot centre. The plot boundary was marked on the ground with spray paint by taping the 28.2 m radius from the plot centre. All trees identified on the aerial photo as green conifers inside the plot boundary were inspected to determine whether they were actually green conifers at the time the photo was taken and whether they were inside the plot boundary. Green conifers in the plot with crown diameters greater than 1 m that were missed during photo interpretation were mapped, assigned new numbers, and later added to the digital stem map.
The following field data were collected on each green conifer in the plot: species, condition, diameter at breast height (DBH), height, crown diameters along north-south and east-west lines, height to base of effective crown, and a judgment of whether it was a future crop tree. The current season's lateral growth of branches was also estimated because crown radii had increased by that amount since the time the aerial photos were made. Likely reasons for each misclassified tree were recorded.
No data were collected on the dead pine overstorey.

2.5 Analysis

During photo interpretation, two conditions had to be met for a tree to be mapped as a green conifer (secondary structure). The interpreter had to judge that it was a green conifer and that its germination point was inside the plot boundary. Both of those conditions had to be verified as correct for the tree to be correctly classified.

The analysis provided answers to the following questions for each interpreted and/or actual green conifer in the plot:

- Was it interpreted on the aerial photo as being in the plot?
- Was it interpreted on the aerial photo as being a green conifer?
- Was it confirmed as being in the plot?
- Was it confirmed as being a green conifer?

Based on the answers, the following results were compiled for each plot:

- Omission errors due to plot boundary
- Omission errors due to tree identification
- Total omission errors
- Commission errors due to plot boundary
- Commission errors due to tree identification
- Total commission errors
- Interpreted number of secondary structure stems in plot
- Actual number of secondary structure stems in plot.

For each tree, a corrected field estimate of crown diameter was calculated by subtracting twice the seasonal crown radius increment from the average crown diameter measured in the field. These were compared with crown diameters measured on aerial photos by linear regression. The

data for trees having interpreted crown diameters greater than 1 m were analyzed separately from those with interpreted crown diameters less than 1 m.

3 Results

3.1 Discrimination of secondary structure

As described in the *Introduction*, the key to this remote sensing method is the reduced ambiguity in the appearance of live understorey fir and spruce trees on winter/overcast aerial photos. This should be readily apparent to a person with experience interpreting aerial photos of forest stands by comparing Figures 1a and 1b. The reason that understory trees are hard to see in Figure 1a is that pixels representing understory trees are not distinct from those representing the forest floor. This is illustrated in Figure 5. Figure 5a shows part of an image taken in the summer during clear conditions. The upper and lower histograms in that figure show samples of pixel values representing spruce crowns and background, respectively. No significance test is required to state that the two populations are no different from one another on the summer photo. Figure 5b shows the same results for the photo taken under winter overcast conditions. On that photo, pixels representing spruce crowns differ so greatly from those representing the background that their classification is clear. The same analysis of the photo taken under winter clear conditions (Figure 5c) shows that spruce crown pixels and background pixels can be discriminated with some confidence but not as well as on winter/overcast photos. The evaluation of winter/clear photos for identifying secondary structure is beyond the scope of this project, but the possible suitability of such imagery would be valuable because it can be acquired by more traditional remote sensing methods, given sufficient resolution and complete snow cover.

The differentiation of tree pixels and background pixels on winter/overcast photos, combined with the distinctive shape of understorey spruce and fir crowns, makes it easier to identify secondary structure and could satisfy the requirements of computer aided pattern recognition, but that is also beyond the scope of this project.

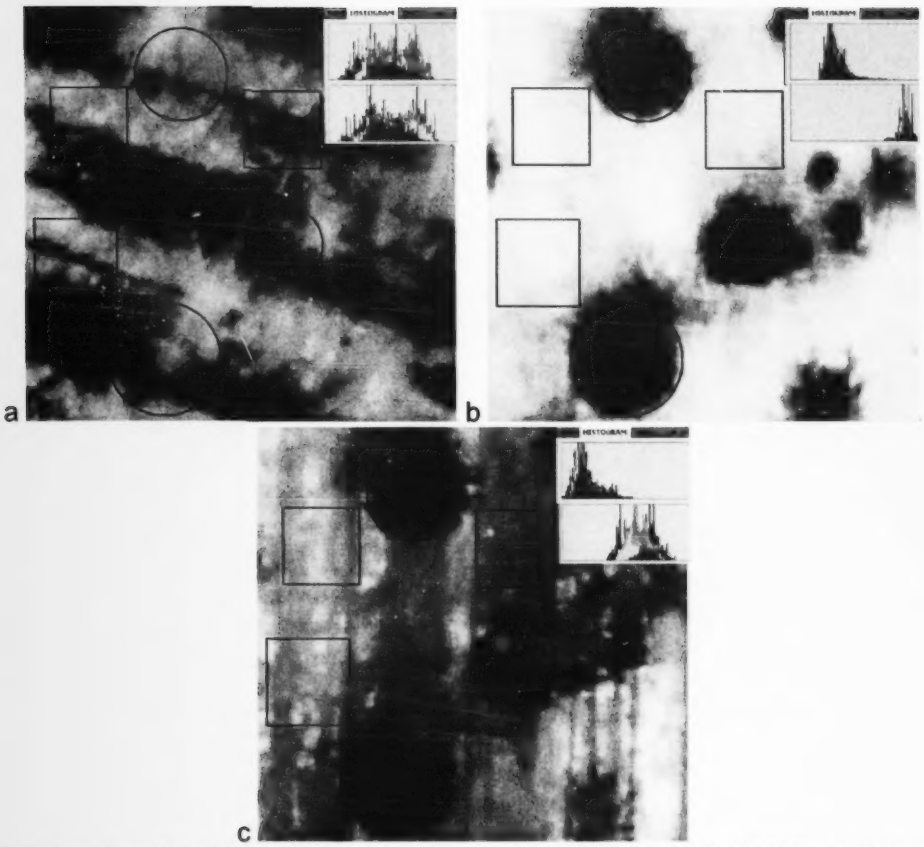

Figure 5. A portion of plot SS04 taken during summer/clear conditions (a: July 2008), winter/overcast conditions (b: March 2008) and winter/clear conditions (c: February 2009). Aggregate samples of pixels representing understorey spruce trees (circled areas) and snow-covered forest floor (squared areas) were taken and frequency distributions were plotted. The upper histogram in each figure represents spruce crowns and the lower histogram represents the background.

3.2 Classification and mapping of secondary structure

Figures 6 and 7 show the SS01 reference image, the plot boundaries, and a map of secondary structure stems. The small circles are the interpreted stems; squares and diamonds represent the omission and commission errors. Figures 8 through 13 show the same information for plots SS02, SS03, and SS04.

The accuracy of secondary structure tree classification is summarized in Table 1. In all four plots, the net counts by photo interpretation were higher than those made in the field, ranging from 3.3% higher to 21.2% higher. These include the net effects of both omission and commission errors, which are further categorized as being due to either inclusion or exclusion of stems at the plot boundary or to tree identification. Omission errors range from 1.3% to 7.7% while commission errors ranged from 11% to 23%. Most errors were due to tree classification rather than to determining whether or not it was inside or outside the plot boundary.

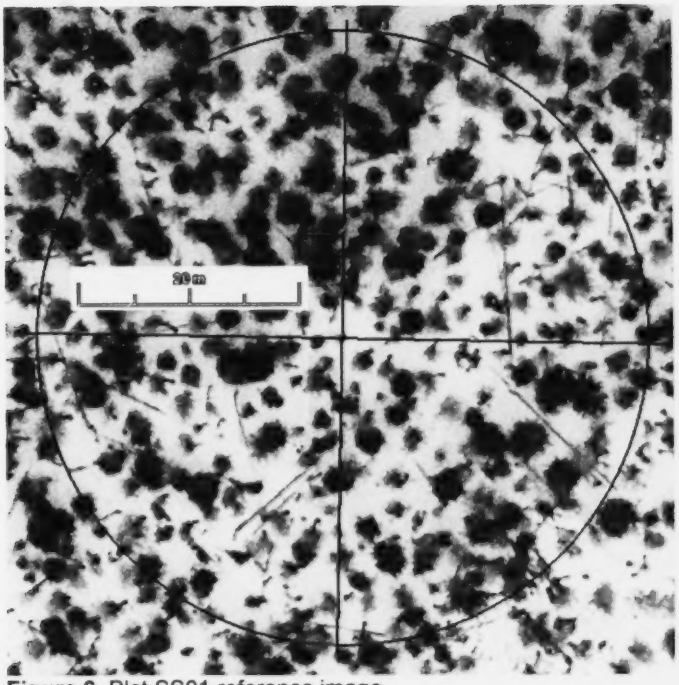

Figure 6. Plot SS01 reference image.

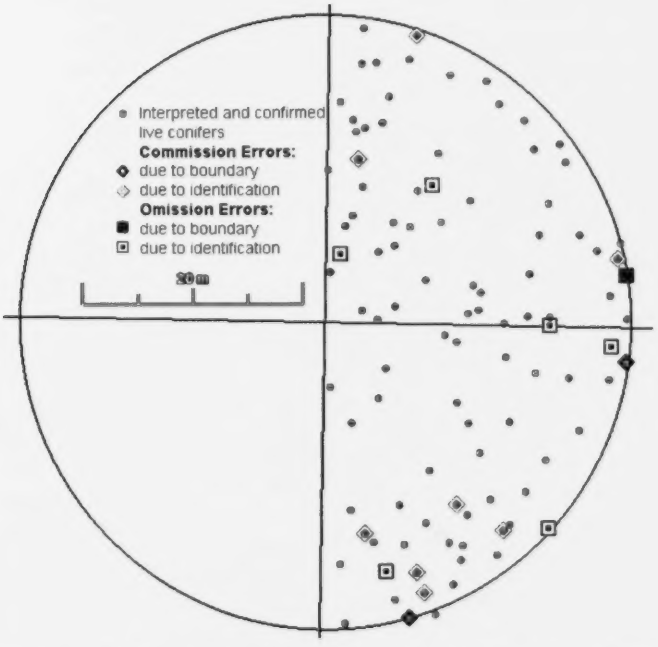

Figure 7. Plot SS01 map of interpreted green conifers and errors of commission and omission.

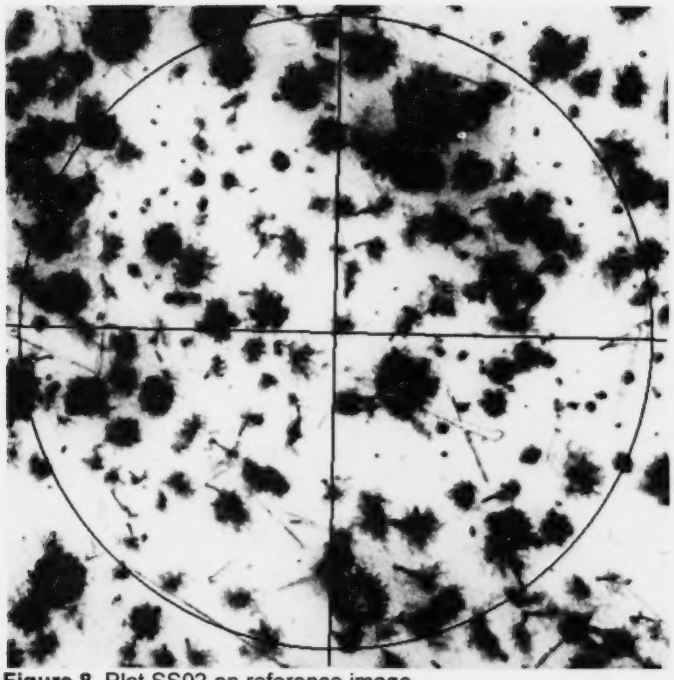

Figure 8. Plot SS02 on reference image.

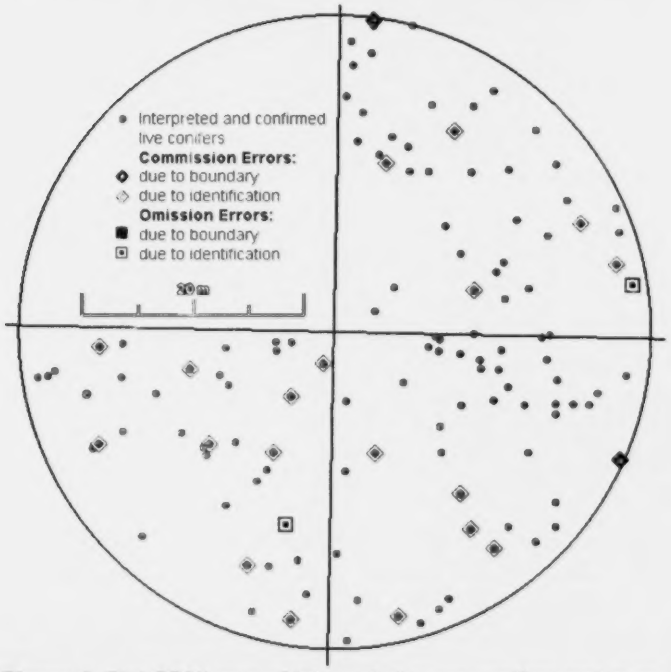

Figure 9. Plot SS02 map of interpreted green conifers and errors of commission and omission.

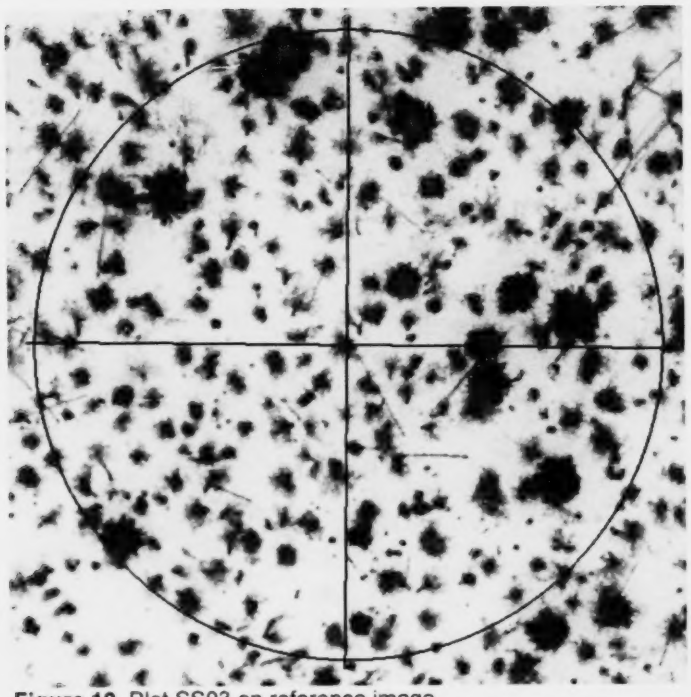

Figure 10. Plot SS03 on reference image.

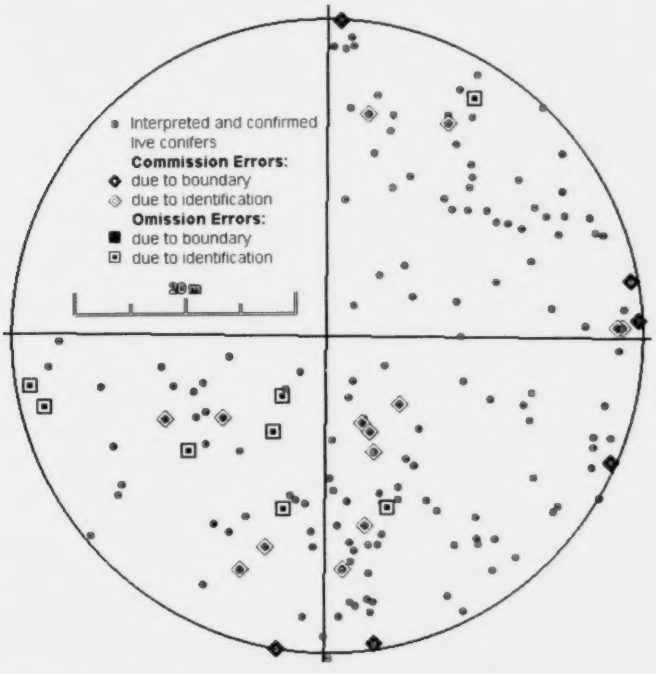

Figure 11. Plot SS03 map of interpreted green conifers and errors of commission omission.

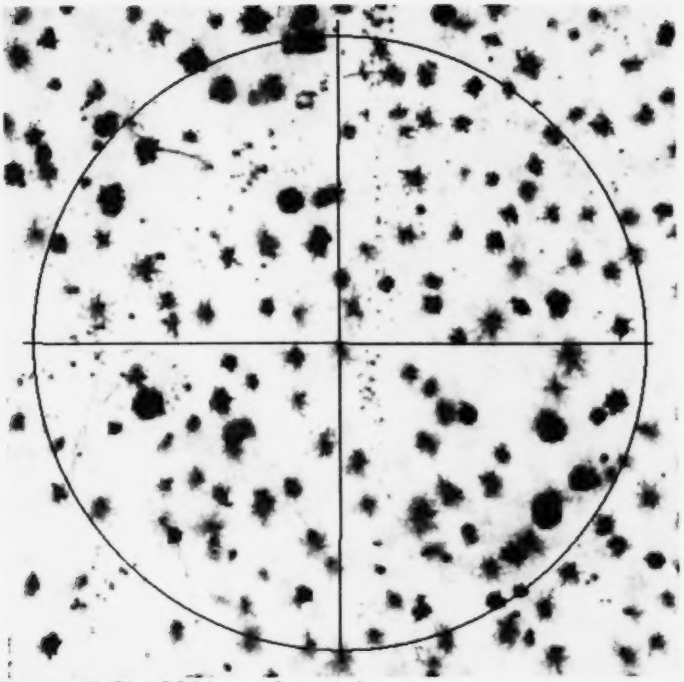

Figure 12. Plot SS04 on reference image.

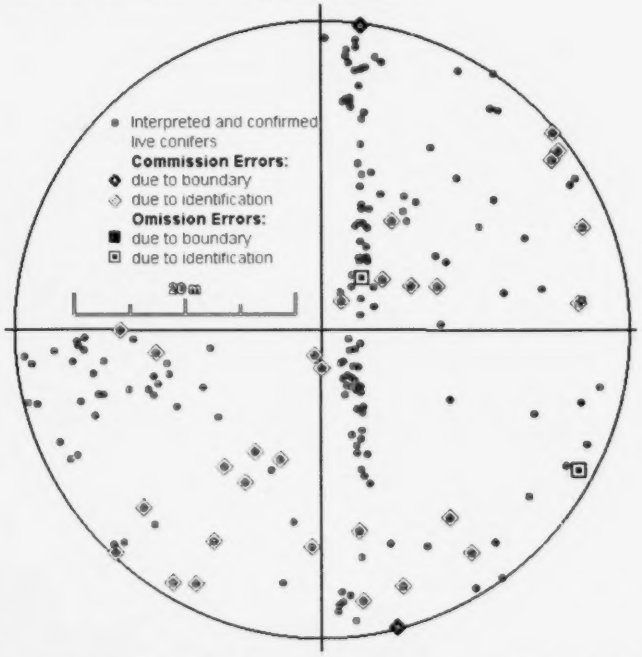

Figure 13. Plot SS04 map of interpreted green conifers and errors of commission and omission.

Table 1. Plot information and summary of secondary structure classification accuracy.

	SS01	SS02	SS03	SS04
BEC subzone	SBPSmk	SBPSmk	SBSdw2	IDFdk3
Plot area (sq. m.)	1250	1250	1875	1875
No. interpreted as secondary structure in plot	94	120	151	184
No. confirmed as secondary structure in plot	91	99	139	155
Individual trees correctly classified on photo	84	97	131	153
Net error in count	3	21	12	29
% error in count	3.3	21.2	8.6	18.7
Omission Errors due to plot boundary	1	0	0	0
Omission Errors due to classification	6	2	8	2
Total Omission Errors	7	2	8	2
Commission Errors due to plot boundary	2	2	5	3
Commission Errors due to classification	8	21	15	28
Total Commission Errors	10	23	20	31
% Omission Error	7.7	2.0	5.8	1.3
% Commission Error	11.0	23.2	14.4	20.0
Total secondary structure stems/ha	728	792	805	981
Total secondary structure >4m stems/ha	656	616	379	667
Total secondary structure >6m stems/ha	520	520	181	613

3.3 Estimation of crown diameters

Figure 14 shows the scatterplots of crown diameters measured in the field (with the 2008 growing season increment subtracted) versus crown diameters interpreted on March 2008 aerial photos. Crown diameter measurements were analyzed in two parts: one for trees with interpreted crown diameters of less than 1 m and one for trees with interpreted crown diameters of greater than 1 m. Crown diameters less than 1 metre were estimated in plots SS02, SS03, and SS04.

Linear regression parameters were calculated on the paired crown diameter measurements for trees interpreted to be greater than 1 m for each of the four plots separately. The results were then tested for differences between regression slopes and intercepts. The P-value of the heteroskedasticity-robust F-test was 0.069. Therefore, the null hypothesis that there was no difference between regressions could not be rejected at the 5% significance level (Ghement 2009). The paired crown diameter data from the four plots were then lumped, re-analyzed, and regression results re-calculated. Figure 15 shows the scatterplot of those data, the regression line, and the y=x line. Tests on the regression parameters indicated that the intercept was significantly different from 0 but that the slope was not significantly different from 1 at alpha=0.05. This means that for trees with apparent crown diameters greater than 1 m, the interpreter tended to underestimate diameters by fixed amounts, rather than by amounts that were proportional to tree size.

For trees with crown diameters less than 1 m (plots SS02 through SS04), separate regression by plot revealed different results and more proportional variability than for trees with crown diameters greater than 1 m. These are shown in Figure 16. In plots SS02 and SS04, the Y-axis intercepts were 0.352 and 0.143, respectively, and were significantly different from 0 at an alpha of 5%. The intercept for the data from plot SS03 was not significant so regression through the origin was appropriate.

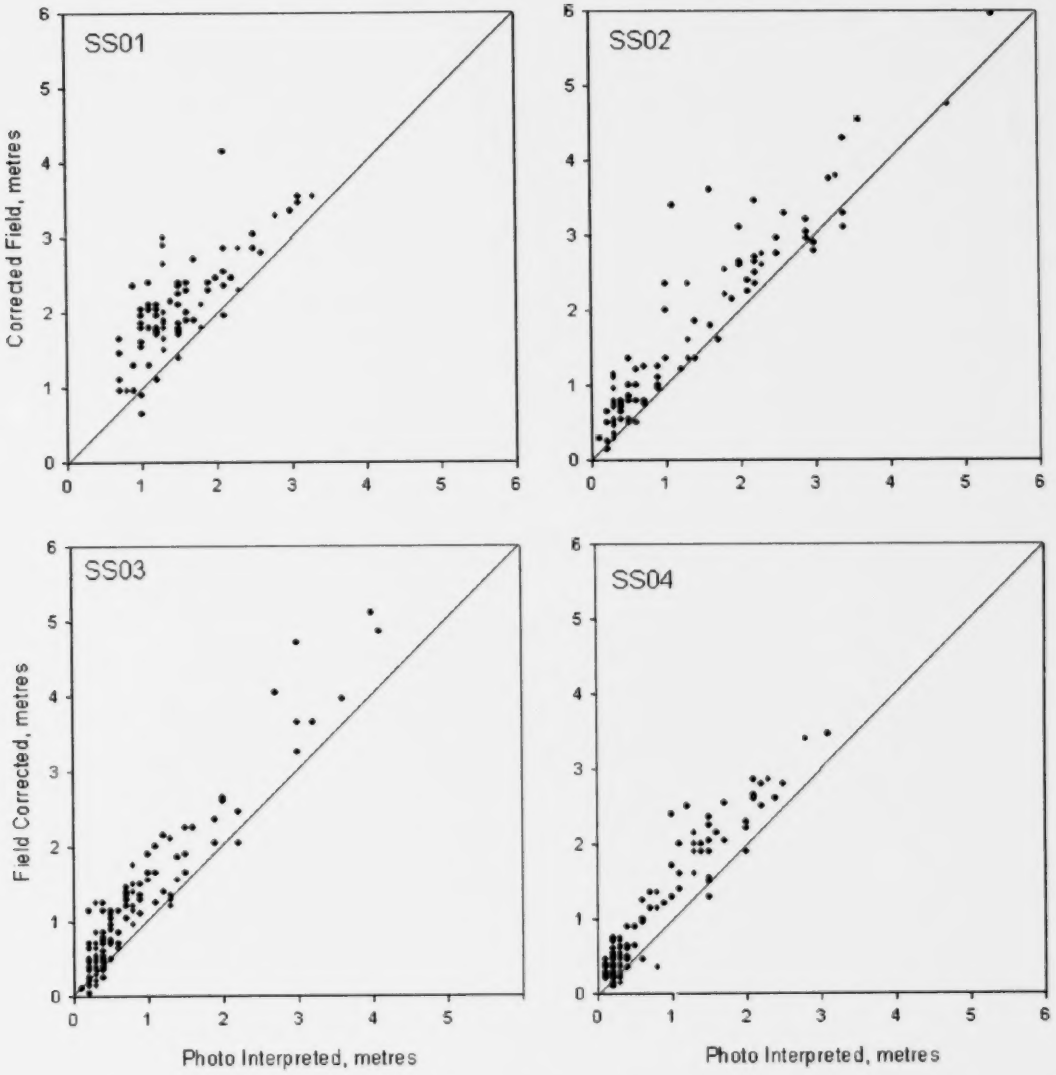

Figure 14. Tree crown diameters measured in the field versus those measured on the georeferenced aerial photo in Google Earth in plots SS01 through SS04.

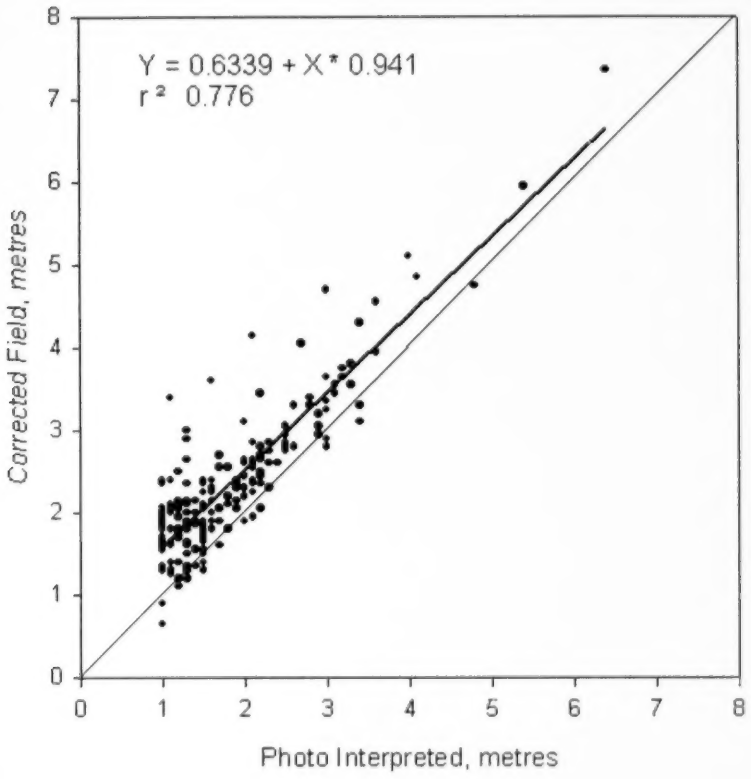

Figure 15. Tree crown diameters measured in the field versus those greater than 1 m as measured on the aerial photos with data from plots SS01 through SS04 merged.

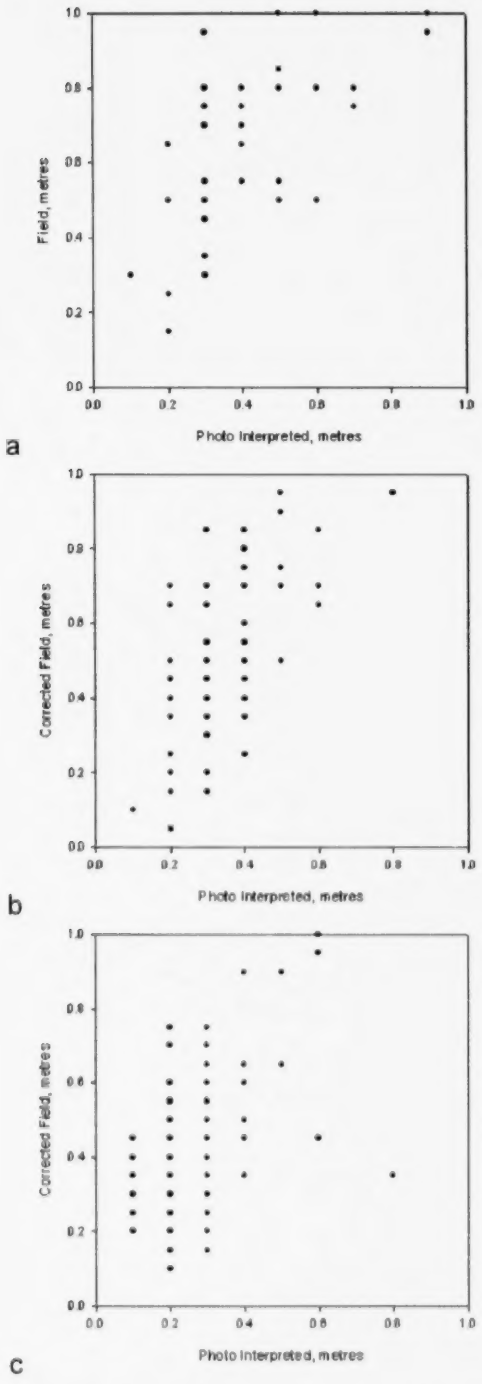

Figure 16. Field- versus photo-measured crown diameters for trees with crowns ≤ 1 m diameter in plots SS02 (a), SS03 (b), and SS04 (c).

3.4 Horizontal scale accuracy

The accuracy of crown diameter estimates on the aerial photos depended on the accuracy of horizontal scale, which in turn depended on the accuracy of georeferencing. Horizontal scale accuracies were determined by comparing horizontal distance measurements between clearly identifiable points on the aerial photos to those measured by a different person in the field. Between three and six measurements were made on each of the four plots over distances of 25 to 40 m. The scatterplot of field-measured distances versus photo-measured distances are shown in Figure 17. Differences ranged from -64 cm to +32 cm in absolute terms and from -2.1% to +1.2% in relative terms. The regression of field measurements versus photo measurements resulted in the following relation:

$$\text{Field Distance, m} = 0.0689\ \text{m} + \text{Photo Distance, m} \times 0.9941$$

with an r^2 of 0.995.

3.5 Operational considerations

There are limitations to acquiring the type of imagery described in this report because snow must cover the forest floor and the sky must be overcast. Snow and frost should also be absent in the forest canopy. Early winter may not provide sufficient snow on the forest floor and mid-winter is problematic because snow or frost are often present in the canopy. Light levels are also low during early- to mid-winter overcast conditions, indicating that late winter provides the best combination of conditions. Flexibility is required for scheduling a photo mission. On any given planned flight day, there is no certainty about conditions until the aircraft is in the air and, on some flights, conditions over a desired target are not known until the aircraft is within five or 10 minutes of the target.

Another limitation is flight altitude, which is constrained by the height of winter cloud bases (often less than 1000 m above ground). The rate of spatial coverage is a function of distance to target, angle of view, and ground speed. At a height of 800 m and with the 60 mm or 105 mm lens on the D200 camera, the swath widths were approximately 200 to 300 m wide, which generated 1 to 2 ha of ground coverage per second. By comparison, a large format film camera mounted in a larger aircraft can acquire ground coverage of similar resolution at a rate 50 to 100 times faster due to a greater aircraft altitude, wider swath width, and higher speed. However, a photo mission utilizing this industry-standard equipment in late winter would only be able to acquire images like that in Figure 1c, not like that in Figure 1b because the mission would have to be flown in clear weather.

The quantitative interpretation method described here required about three person days per plot for georeferencing and producing the stem map and measurements. An alternative use of the images would be to simply categorize photos of beetle-attacked pine stands as having low, medium, or high amounts of secondary structure. An interpreter can inspect the non-georeferenced digital photos and make notes with reference to the photo numbers and flight line maps. This might be useful for stratifying areas for more detailed photo interpretation or field work. With some training, photos could be analyzed at a ground coverage rate of approximately 10 ha per minute.

The only other known method for sampling secondary structure requires ground crews. Therefore, the method described herein could become a useful tool in a multi-scale sampling and inventory program.

4 Discussion and Conclusions

4.1 Detection, classification, and mapping of secondary structure

The photo interpreters made two important conclusions. First, that it was feasible to identify residual green fir and spruce trees in beetle-attacked pine stands by interpreting photos taken during winter overcast conditions. Second, that the potential for making moderately accurate stem maps of secondary structure from aerial photos was unprecedented. They did not know of any other remote sensing product which could match winter/overcast aerial photos for this purpose. The consistent differentiation of live fir and spruce pixels from background pixels was confirmed by preliminary quantitative analysis (Figure 5b). Since understorey fir and spruce trees have a distinct shape as well as relatively consistent pixel value differentiation, it might be feasible to automate part of this process.

The accuracy of identifying residual green conifers was described by summarizing errors of omission and commission, each of which was subdivided into errors due to inclusion/exclusion at the plot boundary and due to tree identification. Misidentified trees were the most common error in all four plots. The most common features to be mistaken for live conifers were dead pine trees, but others included alder bushes and woody debris.

4.2 Crown diameters estimated on aerial photos

The horizontal scales of images used by the interpreters completely depended on the visual georeferencing to the underlying orthophotos. Considering the accuracy of the horizontal scales in the georeferenced photos (Figure 17), the georeferencing must have been at least as accurate. This indicates that errors in estimating crown diameters were due to something other than the accuracy of the horizontal scale of the photos.

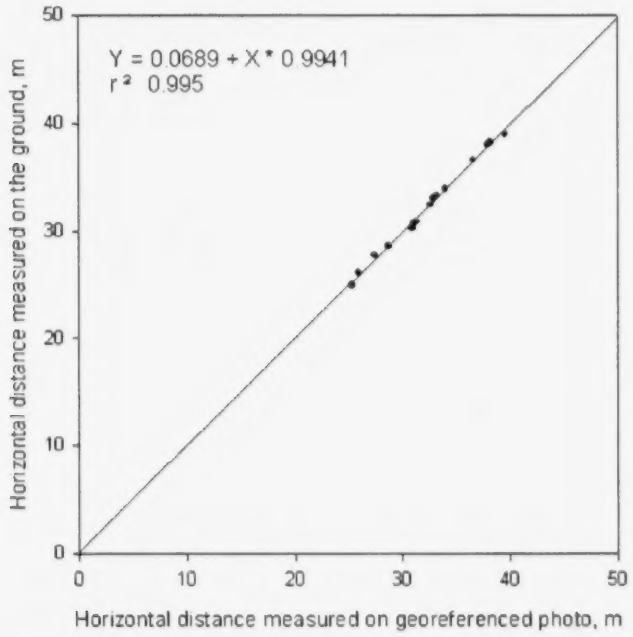

Figure 17. Distances between ground features on the four plots made in the field (y) and estimated on the georeferenced aerial photos (x). Regression line is shown.

The possibility was investigated that tree crowns were actually smaller in March when the photos were taken than they were later when field-checking was done due to low turgor or seasonal deformation of branches by snow press. Plot SS03 was visited in May 2009 about two weeks after the snow had gone. At that time, the tips of understorey fir and spruce branches were essentially perpendicular to the branch nodes, which meant that the vertical projection of crowns would be at their maximum horizontal extent and that there was no crown contraction due to branch droop. For branch droop to cause the underestimated crown diameters, one-metre long branches that were perpendicular to the stem at the time of field-checking would have had to be drooping by more than 40 degrees when the photos were taken.
Reproducibility of the field measurement of crown diameters was also checked in May 2009 by having a different field crew measure the diameters of 10 secondary structure tree crowns. The results indicate a good agreement between the two sets of operators (Figure 18).

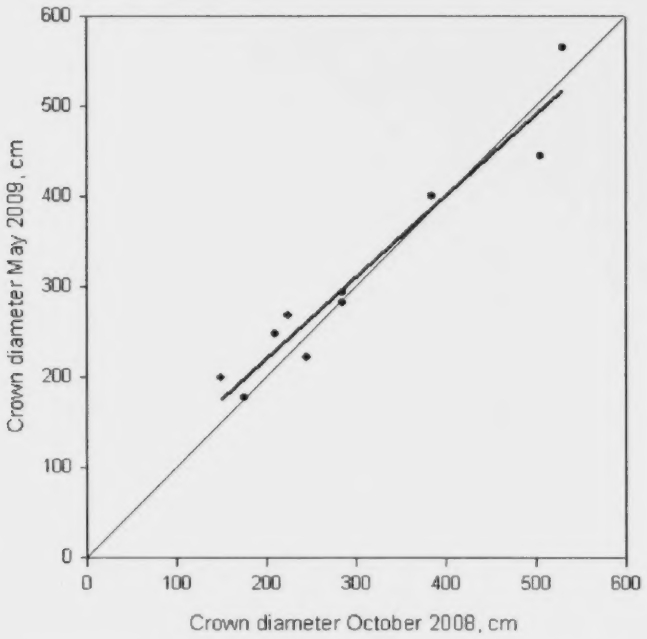

Figure 18. Comparison of crown diameters measured in the field by one crew in October 2008 and by another in May 2009. The y=x line and regression line are shown.

The high accuracy of horizontal scales of georeferenced photos (Figure 17) and good reproducibility of crown diameter measurements in the field suggest that crown diameters might have been underestimated due to misinterpretation of the locations of crown perimeters. To explore this possibility, the two types of measurements were compared for a selection of individual trees as follows. Three understorey fir or spruce trees with crown diameters of 1.25 to 3.75 m (field measurements) were selected in each of the four plots. Dimension arrows representing the crown diameters measured by the two methods were superimposed on the reference images, which were then cropped. The results are shown in Figure 19. Inspection of individual trees and crown diameter measurements by the two methods suggests that the underestimation of crown diameters was greatest in cases where tree perimeters were most irregular or crenulated (e.g. the middle trees in the first, second, and third rows). In some cases, crown diameters were underestimated even though the perimeters did not appear to be irregular,

such as the first tree in the second row and the second tree in the fourth row, possibly because image resolution prevented tips of individual branches from being accurately represented. Since images of the crowns do not appear to be inconsistent with the field measurements of their diameter, operator training in the future may compensate for the tendency to underestimate.

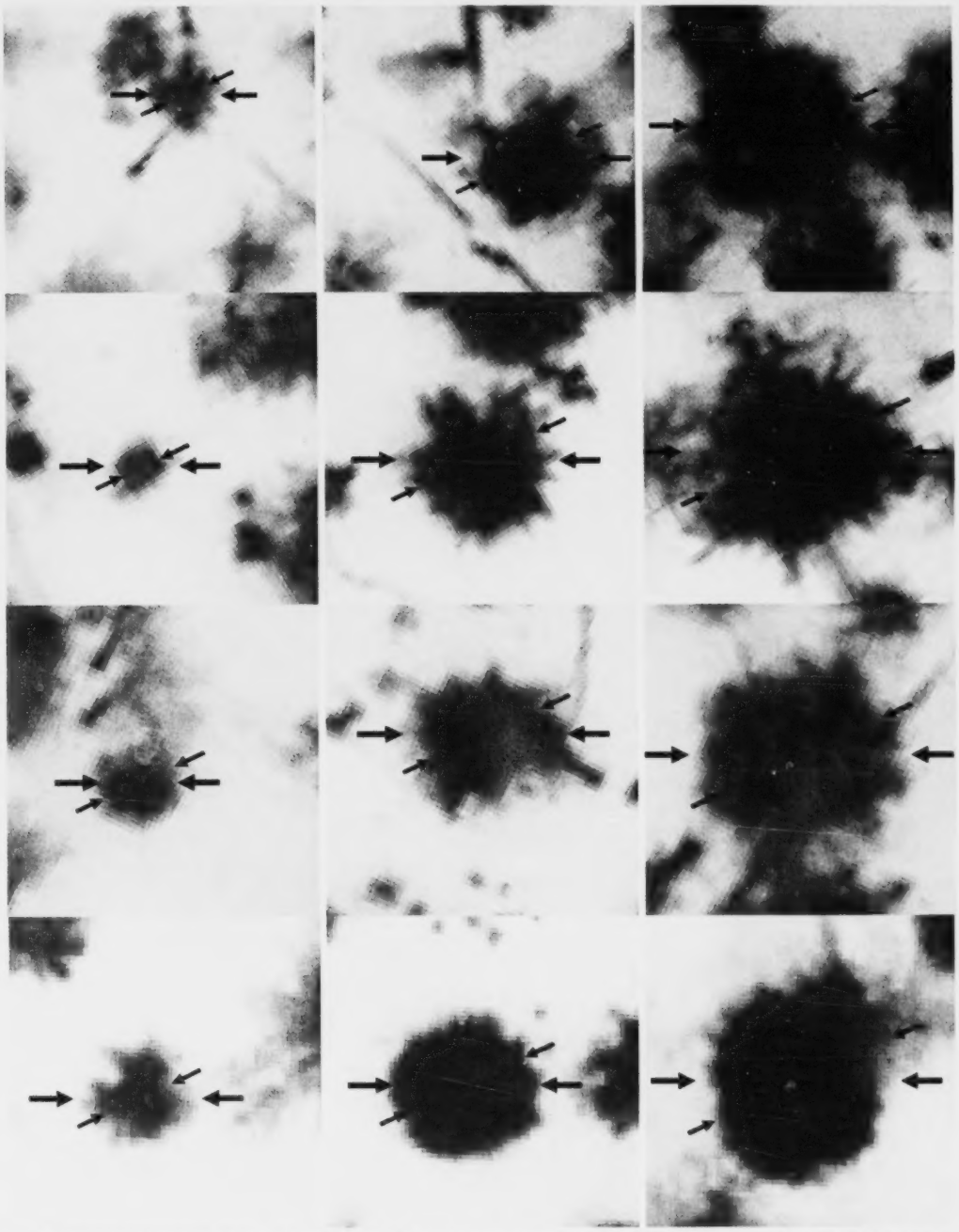

Figure 19. Cropped images of some understorey fir and spruce trees in plots SS01 (top row) through SS04 (bottom row) showing diameters of individual crowns measured on photos (smaller arrows) and in the field (larger arrows).

One photo interpreter described it this way:

> Although the intent was to measure crown width to the branch tips, resolution levels often made it hard to see this on the imagery. It was less difficult if the tip foliage was dense enough with an even edge, but crown perimeters typically have irregularly long branch tips which were hard to see on the photo even though clearly evident when on the ground. The problem is occasionally accentuated by single branch tips jutting out beyond the crown perimeter. Due to the indistinct crown edges at current image resolution levels, it is highly probable my crown width measurements will be underestimated. (Schellenberg pers. comm.)

The results for trees with crowns less than 1 m in diameter are not inconsistent with the results for trees greater than 1 m in diameter but they confirm what is apparent when trying to interpret such small trees on these aerial photos; that is, they are too small to be clearly interpreted.

4.3 Results in relation to the secondary structure regulation

As noted above, this type of aerial photography could be used to classify the abundance of secondary structure without making stem maps. To do so requires a reference set of images showing different amounts of secondary structure confirmed on the ground. The images and data created in this project provide a start to such a reference. Although none of the sampled plots met the criteria in British Columbia's Forest Planning and Practices Regulation for protecting secondary structure (700 stems/ha at least 6 m tall or 900 stems/ha at least 4 m tall, BCMoFR 2009), plots SS01 and SS04 had more than 650 live conifer stems greater than 4 m tall per hectare, which is more than two-thirds of the stem density in the regulation. Plot SS03 had a density of 379 stems of that size class per hectare. Therefore, the four plots in this sample provide examples of secondary structure abundances that range from much less to slightly less than the regulatory requirement.

4.4 Software platform and interpretation methods

The photo interpreters concluded that Google Earth was a convenient platform for interpreting images. Once they got used to it, sequential viewing of overlapping images was an effective way to visualize three-dimensional forest structure. Two advantages are that all interpretation can be done on a computer screen and that the software is free. If stereo interpretation is desired, the overlapping aerial photos can be printed and viewed in traditional ways.

5 Acknowledgements

Ian Moss, R.P.F., was an enthusiastic supporter of this project from its conception. Don Skinner and Kelly Sherman, R.P.F., tested an earlier version of the photo interpretation procedure. Bruce Schellenberg, R.P.F., and David Majcher, R.P.F., interpreted photos and field-checked the work reported here and provided valuable input on the field and office procedures.

This project was funded by the Government of Canada through the Mountain Pine Beetle Program administered by Natural Resources Canada, Canadian Forest Service. Publication does not necessarily signify that the contents of this report reflect the views or policies of Natural Resources Canada, Canadian Forest Service.

6 Contact

Pat Teti, Hydrologist
B.C. Ministry of Forests and Range
200 – 640 Borland Street
Williams Lake, B.C. V2G 4T1
Pat.Teti@gov.bc.ca

7 Literature Cited

Coates, K.D.; DeLong, C.; Burton, P.J.; Sachs, D.L. 2006. Abundance of secondary structure in lodgepole pine stands affected by the mountain pine beetle. Report for the Chief Forester. Accessed September 2009. www.for.gov.bc.ca/hfp/mountain_pine_beetle/stewardship 18p.

de Montigny, L.; Nigh, G.; Archer, R. 2007. MPB stewardship research strategy implementation framework. BC Ministry of Forests, Research Branch, Victoria, B.C. Accessed June 2009. www.for.gov.bc.ca/hre/pubs/docs/mpbstrategy.pdf 28 p.

Ghement, I. 2009. Comparing a field method and a photo interpretation method for measuring tree crown diameters. Draft report prepared for BC Ministry of Forests and Range. 17 p.

(BCMoFR) BC Ministry of Forests and Range. Forest Practices Branch. Accessed June 2009. http://www.for.gov.bc.ca/hfp/silviculture/Silviculture_Surveys.html.

Schellenberg, B. 2009. Sampling secondary structures in beetle-killed pine stands. Contract report to BC Ministry of Forests and Range, June 15, 2009. 4p.